Catal Lett (2016) 146:35–46
DOI 10.1007/s10562-015-1656-7

Vapor Phase Oxidation of Benzyl Alcohol over Nano Au/SBA-15 Catalysts: Effect of Preparation Methods

Ashish Kumar[1,2] · Vanama Pavan Kumar[2] · Amirineni Srikanth[2] · Venkataraman Vishwanathan[3] · Komandur V. R. Chary[2]

Received: 28 April 2015 / Accepted: 9 November 2015 / Published online: 9 December 2015

Abstract Au/SBA-15 nano catalysts were synthesized from four different methods, viz., homogeneous deposition–precipitation, micro-emulsion, impregnation and polyol, and their catalytic activities were investigated for the vapor phase oxidation of benzyl alcohol to benzaldehyde. The physico-chemical properties of the catalysts were characterised by XRD, TEM, BET surface area, pore size distribution, CO-chemisorption and XPS techniques. The structural data of the catalysts along with their catalytic studies indicate that the presence of very small metallic Au^0 species with particle size of 7–8 nm, was responsible for the higher activity observed in the vapor phase oxidation of benzyl alcohol reaction. The title reaction, though industrially important, was used as a test reaction to investigate firstly, the influence of different preparation methods on the uniform dispersion of gold particles on the support SBA-15 and to understand the metal-support interaction in Au/SBA-15 catalysts, and secondly, to study the catalytic performance of the catalyst (Au/SBA-15) in terms of activity, selectivity and stability over a period of reaction time. The conversion of benzyl alcohol was found to increase with decrease in the size of gold particles. Smaller gold particles with higher percentage of dispersion on the support SBA-15 had a beneficial effect on the catalytic activity. Among the four methods used for the preparation of gold on SBA-15 support, the catalyst prepared by homogeneous deposition–precipitation method showed the best performance in terms of conversion, selectivity for benzaldehyde and longer catalyst life.

Graphical Abstract Vapor phase oxidation of benzyl alcohol over nano Au/SBA-15 catalysts.

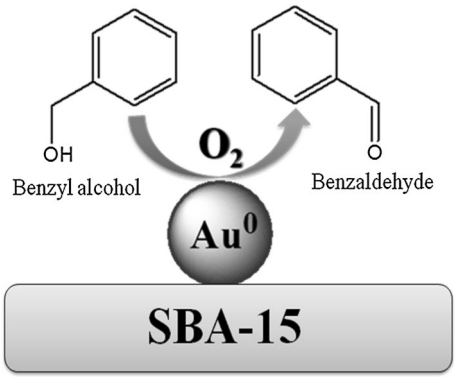

Keywords Gold nanoparticles · SBA-15 · Benzyl alcohol · Oxidation · Benzaldehyde

1 Introduction

It was well established that the catalytic activity of supported gold nanoparticles depends on the particle size, the nature of support and the preparation method. Among the oxidation reactions, the vapor phase oxidation of benzyl alcohol ($PhCH_2OH$) to benzaldehyde (PhCHO) is commercially of importance, since the process is environmentally benign and needs less expensive additives.

✉ Komandur V. R. Chary
kvrchary@iict.res.in

[1] School of Chemistry and Biochemistry, Thapar University, Patiala 147004, India

[2] Catalysis Laboratory, Inorganic & Physical Chemistry Division, CSIR-Indian Institute of Chemical Technology, Hyderabad 500007, India

[3] Department of Chemistry, Sreyas Institute of Engineering and Technology, Hyderabad 500068, India

Conventionally, benzaldehyde was produced as a by-product during the oxidation of toluene ($PhCH_3$) to benzoic acid (PhCOOH) or from the hydrolysis of benzyl dichloride. But, these reaction routes are known to promote a large amount of hazardous by-products like organic chlorine or benzoic acid. Hence, this limits the usage of benzaldehyde in the cosmetics, pharmaceutical and flavouring industries [1]. From the commercial view, air or molecular oxygen is the favourite choice as the primary oxidant since they produce water as the by-product [2]. However, the use of air requires the development of newer and novel catalysts in order to achieve higher catalytic activity under ambient reaction conditions. Many studies have employed in the recent past on the supported gold as catalysts in several catalytic applications including selective aerobic oxidation of alcohols such as benzyl alcohol [2–4]. In order to achieve a high catalytic performance, these catalysts are employed in the form of nano-composites where nanoparticles of gold are loaded onto the support materials like activated carbon, metal oxides and polymers. However, such batch reactions in liquid phase require a longer period of time to reach the steady state and also require the separation of catalysts from the products. From the viewpoint of atom economy and green chemistry, the emphasis has been laid more on the vapor phase catalytic oxidation of benzyl alcohol to benzaldehyde [1, 4–8], since it is solvent free continuous and provides a higher selectively for benzaldehyde. Recently, Rossi et al. [3, 8] have reported that gold catalysts to be more effective in the vapor phase oxidation of volatile alcohols to form the corresponding ketones and aldehydes.

Mesoporous SBA-15 materials exhibit several unique characteristics such as high surface area, long range ordering of mesoporous channels, larger pore volume and their high pore wall thickness which provides good thermal and hydrothermal stability as well as improved acid–base tolerance [9–11].

In recent years, nano-sized gold particles have been reported to show a higher catalytic activity [12–15]. We have reported recently similar studies over Ru/SBA-15 catalysts synthesized from different methods viz., microemulsion (ME), polyol (POL), impregnation (IMP) and deposition–precipitation method [16]. The superior catalytic behaviour is attributed to the formation of nanoparticles of ruthenium over mesoporous SBA-15. The nanostructure gold catalysts prepared in present work by the homogeneous deposition–precipitation (HDP) using urea as the precipitating agent has shown superior activity for benzyl alcohol oxidation compared to the catalysts derived from other methods. The HDP method has several advantages such as simple, facile, better control of pore structures and of higher dispersion of gold nanoparticles at low concentration on the catalyst support [12].

The present investigation deals with the preparation of Au/SBA-15 nano-catalysts from four different routes, namely, homogeneous precipitation-deposition, ME, IMP and POL. Here, we report the unique structural features of SBA-15 materials as a support for preparing active catalyst for producing benzaldehyde by vapor phase oxidation of benzyl alcohol. Investigation of these catalysts in the oxidation of benzyl alcohol under vapor phase conditions resulted in a good stability in terms of conversion and higher selectivity towards the formation of benzaldehyde. The importance of vapor phase reaction is well known since it can be performed continuously at moderate reaction conditions with higher selectivity of the desired product as compared to the liquid phase reactions.

The structural features of Au/SBA-15 catalysts were investigated by XRD, TEM, BET surface area, PSD, CO-chemisorption and XPS techniques. A comparative study has been made with respect to their structural properties, oxidation activity and selectivity for benzaldehyde.

2 Materials and Methods

2.1 Catalyst Preparation

2.1.1 Preparation of Mesoporous SBA-15 Support

Mesoporous SBA-15 was prepared by the procedure described elsewhere [9–11]. Briefly, the procedure consist of dissolving 2.0 g of triblock copolymer Pluronic P-123 template with stirring in a solution of 15 g of water followed by adding 45 g of 2 M HCl at 40 °C. Further, about 5.9 g of tetraethylortho-silicate (TEOS) (Sigma-Aldrich, 99.8 %) was added dropwise in the homogeneous solution with stirring. The molar ratios of TEOS:HCl:H_2O:polymers were maintained as 1.0:3.1:115:0.012, respectively. The synthesis mixture was continuously stirred at 40 °C for 20 h, and finally hydrothermally treated at 98 °C for 24 h in an oven. The as-prepared solid product was separated by filtration, washed with deionized water and ethanol to remove the excess of template and dried in air at room temperature for 12 h. The organic template was removed by calcination in air at 550 °C for 5 h.

2.1.2 Preparation of Gold Catalysts

The Au/SBA-15 catalysts were prepared by four different preparation methods: HDP, ME, IMP and POL, using $HAuCl_4{\cdot}3H_2O$ (Sigma-Aldrich, 99.8 %) as metal precursor. Prior to characterization and catalytic activity measurements, all the catalysts were chemically reduced by 0.1 M, freshly prepared $NaBH_4$ aqueous solution and calcined at 400 °C for 3 h in N_2 atmosphere. The EDAX-

analysis showed that the presence of sodium was negligible (<0.01 %).

Homogeneous Deposition–Precipitation (HDP) Method The Au/SBA-15 catalyst was prepared by HDP method using urea as the precipitating agent [12, 17]. The mixture of an aqueous solution containing $HAuCl_4{\cdot}3H_2O$ (Sigma-Aldrich, 99.8 %, with desired gold loading) and urea was stirred with gradual heating to a temperature up to 95 °C for 6 h. On heating, the urea decomposes to give ammonia and hence precipitation occurs in a homogeneous way in the whole bulk solution as the pH shift towards basic conditions (pH 6–8). Than after, the mesoporous SBA-15 was added to the above solution with continuous stirring. The solid product was filtered, washed thoroughly with deionized water until the filtrate contained no chloride ions (confirmed with $AgNO_3$ test) and subsequently dried in hot air oven at 100 °C for 5 h.

Micro-Emulsion (ME) Method The sample prepared by this method was described briefly in the following method [18, 19]. In container-A, 0.5 g of cetyltrimethyl ammonium bromide (CTAB), 5 mL of n-butanol and 30 mL of cyclohexane were added together and stirred until a clear solution was obtained. In container-B, an aqueous solution containing $HAuCl_4{\cdot}3H_2O$ (0.086 g) precursor and 110 mL of tetrahydrofuran (THF) were made. Now, the solution of container-B was added to the container-A along with the required amount of SBA-15 support. The solid product formed was filtered and washed with THF to remove the surfactant completely. The filtrate was further washed with ethanol and subsequently dried in hot air oven at 100 °C for 5 h.

Impregnation (IMP) Method The Au/SBA-15 catalyst was prepared by impregnating of SBA-15 with an aqueous solution of $HAuCl_4{\cdot}3H_2O$ [20, 21]. The required amount of $HAuCl_4{\cdot}3H_2O$ (0.086 g) solution was added to the SBA-15 support and the mixture was then stirred for 4 h. The mixture was finally dried at 50 °C for 4 h in a rotary evaporator.

Polyol (POL) Method The Au/SBA-15 catalyst was prepared by using the following method [22]. Approximately 20 mL of ethylene glycol was placed in an ice bath and required amount of SBA-15 support was added to it. In another container, 0.086 g of $HAuCl_4{\cdot}3H_2O$ was dissolved in 10 mL of ethylene glycol separately. The above solution was added drop wise to 20 mL ethylene glycol in an ice bath with constant stirring for 20 min. The final mixture was allowed to settle. The filtrate was washed with ethanol and subsequently dried at 100 °C for 5 h.

2.2 Catalysts Characterization

X-ray powder diffraction (XRD) patterns of the catalysts were recorded on a Rigaku Miniflex (M/s. Rigaku Corporation, Japan). X-ray diffractometer using Ni filtered Cu Kα radiation (λ = 0.15406 nm) with a scan speed of 2° min^{-1} and a scan range of 10°–80° for wide angle diffraction at 30 kV and 15 mA. The crystallite size of gold was calculated by using Debye–Scherrer equation and phase identification with the help of the JCPDS files.

The CO-chemisorption measurements were carried out on AutoChem 2910 (Micromeritics, USA) instrument. About 100 mg of the catalyst was pre-treated with helium gas for 1 h at 150 °C. The sample was subsequently cooled to 50 °C in the same He gas stream. CO uptake was determined by injecting pulses of 10 % CO/He from a calibrated online sampling valve into the He gas stream passing over the samples at 80 °C. Metal area, metal

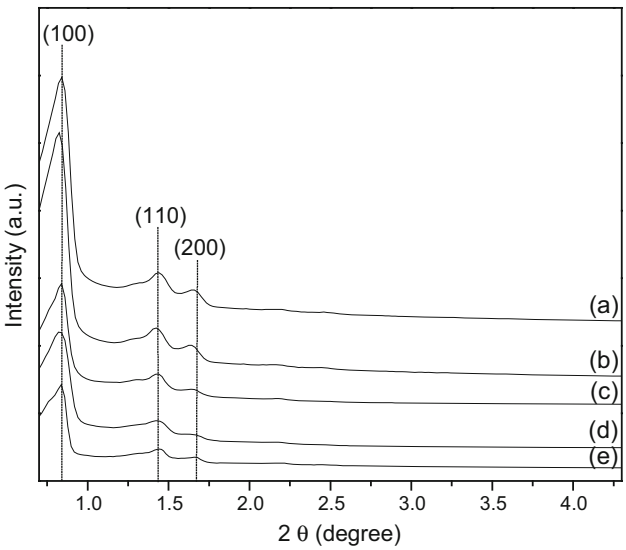

Fig. 1 Low angle XRD patterns of *a* SBA-15 and Au/SBA-15 catalysts, *b* HDP, *c* ME, *d* IMP and *e* POL

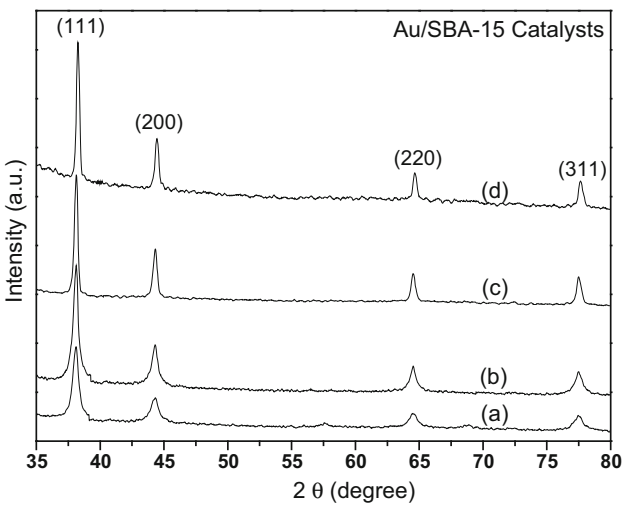

Fig. 2 Wide angle XRD patterns of Au/SBA-15 catalysts. *a* HDP, *b* ME, *c* IMP and *d* POL

dispersion and metal average particle size were calculated assuming the stoichiometric factor (CO/Au) as 1. Adsorption was deemed to be completed after three successive runs showed similar peak area.

Gold content was determined by inductively coupled plasma optical emission spectrometer (ICP-OES) on a Varian 720-ES instrument. Solid samples were first digested in a mixture of HF, HCl, and HNO_3 in a microwave oven for 2 h and further diluted with deionised water to analyze the gold contents by ICP-OES. ICP analysis, performed on the fresh samples of Au/SBA-15 catalysts.

The BET surface areas of the catalysts were obtained from N_2 adsorption–desorption isotherm (Autosorb I/Quantachrome instruments, USA at −196 °C). The samples were first out gassed at 300 °C to ensure a clean surface prior to nitrogen adsorption. The Barrett–Joyner–Halenda (BJH) method was used to calculate the pore-size distribution from the desorption branch of the isotherm (Autosorb I/Quantachrome, USA).

Transmission electron microscopy (TEM) images of the catalysts were obtained using a Technai-12, FEI, Netherlands at an accelerating voltage of 120 kV. The specimens were prepared by dispersing the samples in methanol using an ultrasonic bath and evaporating a drop of resultant suspension onto the carbon coated copper grid.

Thermo gravimetric analysis (TGA) is used to measure the heat flow and rate change as a function of temperature or time of the catalysts. The TGA analysis of the catalyst was measured on a Q500, TA instruments, USA.

X-ray photoelectron spectroscopy (XPS) is used to study the chemical composition and oxidation state of catalyst surfaces. The XPS spectra of the catalysts were measured on a XPS spectrometer (KRATOS Axis 165, Shimadzu, UK) with Mg Kα radiation 1253.6 eV at 75 W. The gold 4f core-level spectra were recorded and the corresponding binding energies referenced to the C 1 s line at 284.6 eV [accuracy within (0.2 eV)]. The background pressure during the data acquisition is kept below 10^{-9} torr.

2.3 Catalytic Activity

A fixed bed vertical down flow glass reactor (length = 520 mm, i.d. = 12 mm) used for the vapor phase oxidation of benzyl alcohol under ambient atmospheric pressure. An amount of 1.0 g catalyst was diluted with an equal amount of same size quartz grains was packed in between two layers of quartz wool. The upper portion of the reactor was filled with glass beads which serve as a preheater for the reactant. Prior to the oxidation reaction, each catalysts were activated at 250 °C for 2 h in the presence of N_2 flow (50 mL/min) to ensure a clean surface of the catalysts. Thereafter, the benzyl alcohol (Sigma-Aldrich, 99.8 %) was fed into the reactor in a stoichiometric quantity (WHSV = 2.84 h^{-1}) using a syringe pump (Perfusor, B. Braun, Germany) by passing air along with the reactant at 320 °C. The reaction products were collected in an ice-cold trap at the bottom of the reactor for every 1 h.

The reaction products were analyzed by a HP-6890 gas chromatograph equipped with a HP-5 capillary column having flame-ionization detector (FID) and the reaction products were also identified by HP-5973 quadruple GC-MSD system with a HP-1MS capillary column using He as a carrier gas. However, the gaseous products were introduced to a 1 cm^3 gas sampler and analyzed by gas chromatography (SHIMADZU GC-2014) equipped with a thermal conductivity detector (TCD) using Carboxen 1000 column, under an Helium as carrier gas.

3 Results and Discussion

3.1 Characterization of Catalysts

The low angle XRD pattern of the SBA-15 and different Au/SBA-15 catalysts are shown in Fig. 1. As can be seen from Fig. 1 the XRD peaks at 2θ = 0.83°, 1.44°, 1.66° corresponds to the planes of (100), (110), and (200) due to

Table 1 The physico-chemical properties of Au/SBA-15 catalysts

S. No.	Au/SBA-15 (1 wt%)	CO_{irr} (μmol/g)	Au dispersion (%)[a]	Am (m^2/g_{cat})[b]	Am (m^2/g_{Au})[c]	d_{Au} (nm)[d]	d_{Au} (nm)[e]	d_{Au} (nm)[f]
1.	HDP	10.73	16.55	0.44	43.99	7.05	6.08	7.36
2.	ME	5.02	9.94	0.27	26.43	11.74	7.87	8.34
3.	IMP	4.97	9.84	0.26	26.15	11.87	8.91	9.44
4.	POL	4.84	9.62	0.25	25.58	12.14	9.68	10.38

[a] Au dispersion

[b] Metal area (catalyst)

[c] Metal area (gold)

[d] Au particle size determined from COirr uptake values

[e] Au crystallite size determined from XRD

[f] Au particle size determined from TEM

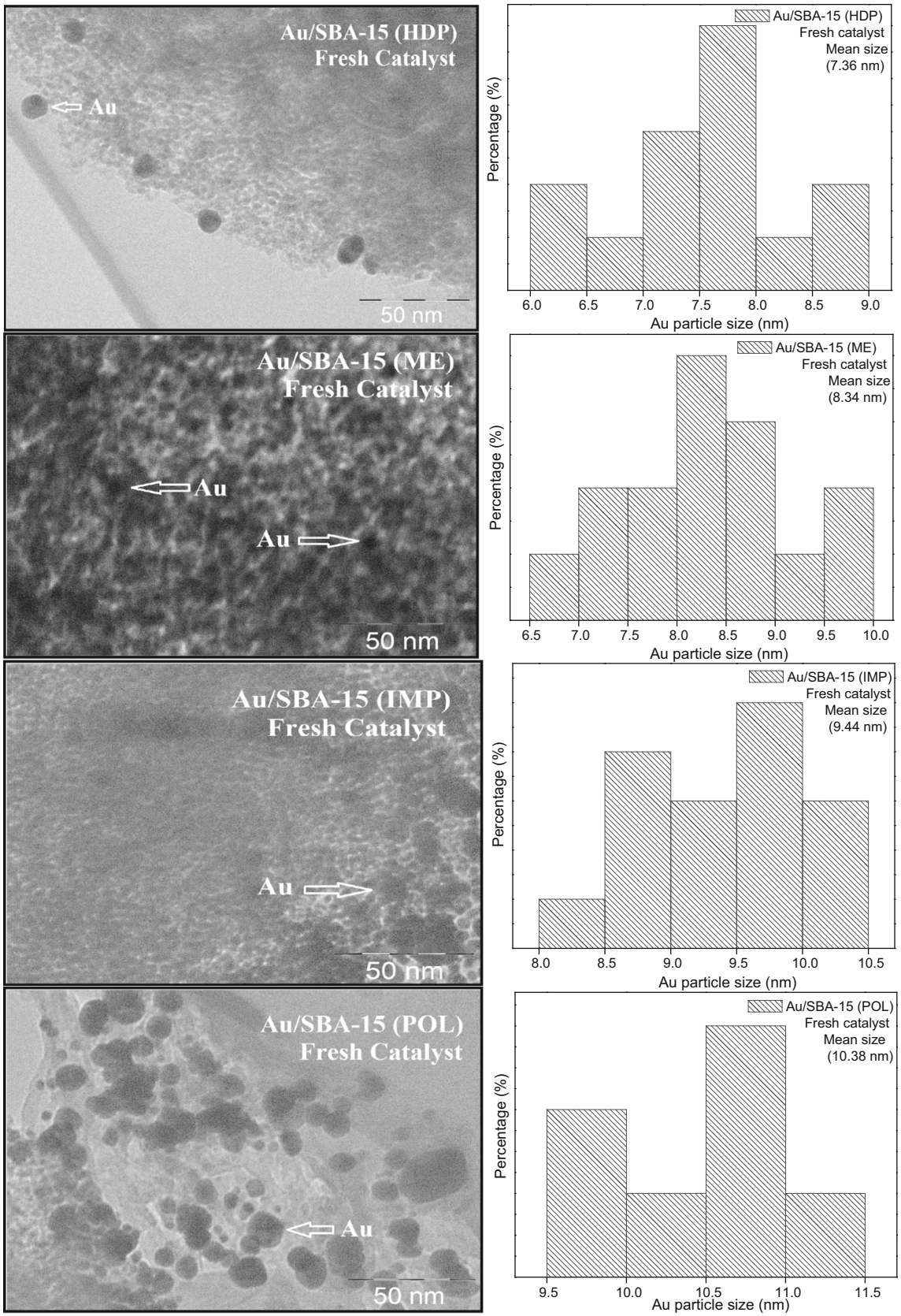

Fig. 3 TEM images and histograms comparing the gold particle size distribution of different Au/SBA-15 catalysts

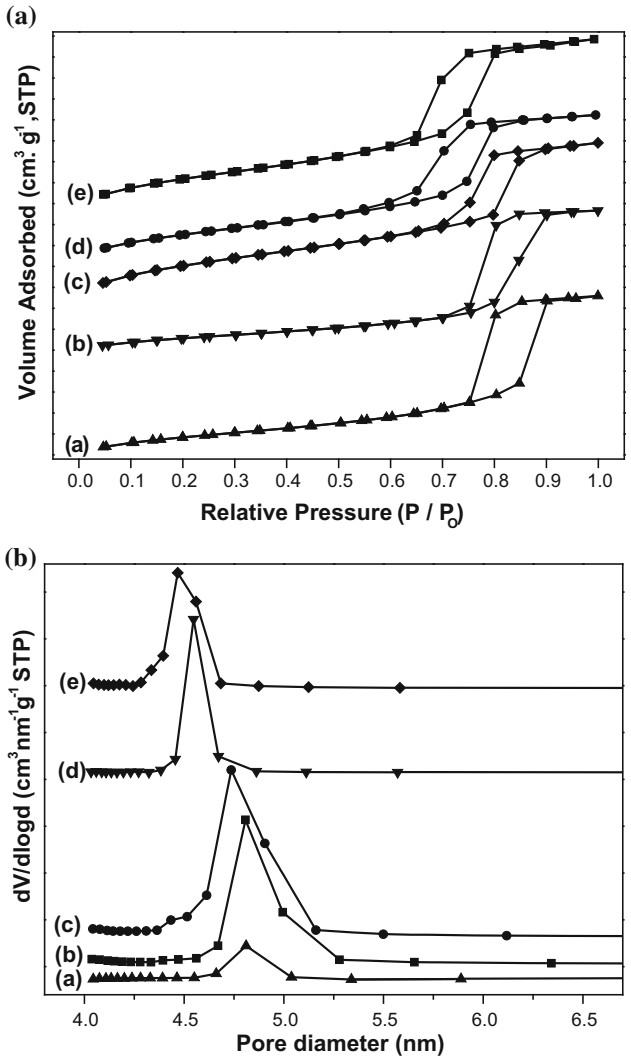

Fig. 4 **a** N_2 adsorption–desorption isotherms for *a* SBA-15 and Au/SBA-15 catalysts, *b* HDP, *c* ME, *d* IMP, *e* POL. **b** BJH pore size distribution for *a* SBA-15 and Au/SBA-15 catalysts, *b* HDP, *c* ME, *d* IMP, *e* POL

the characteristic peaks of mesoporous structure of SBA-15 [10]. The Braggs reflections, confirm the hexagonal symmetry (P6 mm) of the SBA-15 material [23]. The XRD patterns of Au catalysts supported on SBA-15 reveals that there were no significant changes observed upon Au loading, indicating that the structure of the SBA-15 was remain intact even after gold deposition. The decrease in the intensity of XRD the peaks at $2\theta = 1.4°$ and 1.6° for the synthesized catalysts are due to blockage of the pores of SBA-15 by Au particles [24].

The wide-angle XRD patterns of 1 wt% loadings of Au catalyst supported on SBA-15 are shown in the Fig. 2. This figure clearly demonstrates that the broad diffraction peak at $2\theta = 22.4°$ are observed for all the Au/SBA-15 catalysts due to the amorphous silica framework of SBA-15. The Au/SBA-15 catalysts exhibits four diffraction peaks at $2\theta = 38.2°$, 44.3°, 64.3°, 77.4° which are indexed to (111), (200), (220), and (311) reflections, respectively, for the face-centred cubic (FCC) lattice structure of Au (JCPDS file number: 04-0784) [24, 25]. However, the mesoporous ordered structure of SBA-15 could be retained even after complete gold deposition, as shown in the Fig. 2. In 1 wt% Au/SBA-15 (HDP) the XRD reflections due to 38.2° and 44.3° are not resolved and appear due to presence of gold nanoparticles (2–3 nm) in amorphous state. However, at lower loadings we could not see the reflections due to metallic gold indicating the presence of gold in a highly dispersed form or the crystallite size could be very low (<4 nm) which was beyond the detection limit of XRD.

The XRD patterns also indicate that there are no characteristic peaks noticed due to the formation of mixed phase due to interaction between Au and SBA-15 support. This indicates the formation of Au^0 phase. The peaks are sharp and intense, indicating good crystallinity of metallic Au and crystallite size for all the gold catalysts were calculated from Scherrer's equation and reported in Table 1.

Table 2 Textural properties of mesoporous SBA-15 and various Au/SBA-15 catalysts

S. No.	Au/SBA-15 (1 wt%)	Au content (wt%)[a]	Surface area (m^2/g)[b]	V_t (cc/g)	D_{BJH} (nm)	Binding energy (eV)	
						$4f_{5/2}$	$4f_{7/2}$
1.	SBA-15	0.00	846	1.75	4.81	–	–
2.	HDP	0.87	762	1.69	4.80	87.59	83.99
3.	ME	0.79	722	1.57	4.73	87.15	83.95
4.	IMP	0.77	681	1.49	4.54	87.13	83.55
5.	POL	0.75	645	1.41	4.47	87.11	83.42

V_t Total pore volume, D_{BJH} average pore diameter calculated by BJH adsorption method

[a] Gold content measured by ICP-OES

[b] BET method

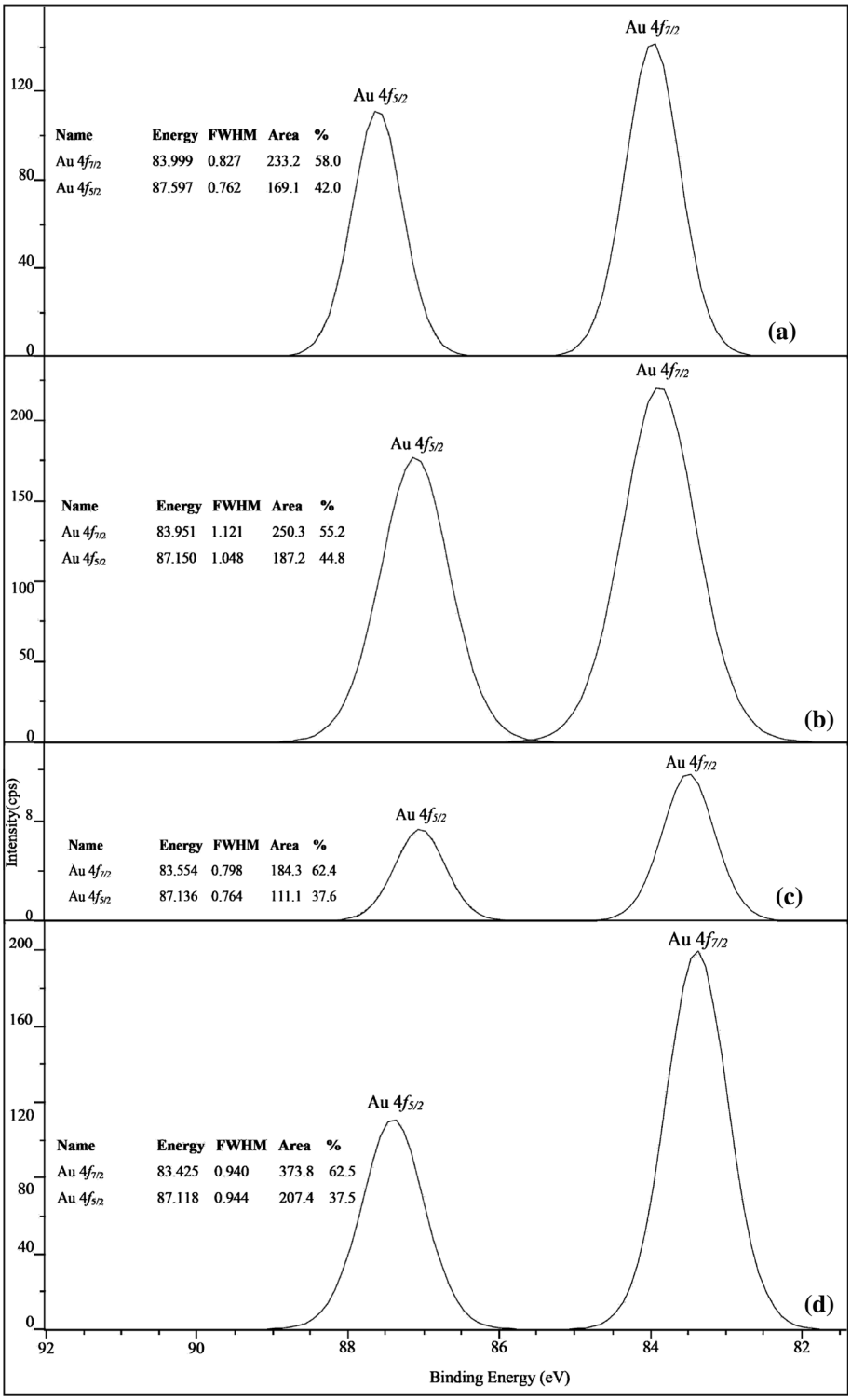

Fig. 5 XPS spectrum of Au/SBA-15 catalysts. *a* HDP, *b* ME, *c* IMP and *d* POL

The physico–chemical properties of Au/SBA-15 catalysts such as dispersion, metal area and particle size were determined from CO-chemisorption and reported in Table 1. From the Table 1, it is evident that the irreversible CO uptake increase for Au/SBA-15 (HDP) catalyst and decreases for others catalyst. It is observed that decrease in CO uptake with increase in particle size as shown in Table 1. This suggests to the agglomerization in turn leads to the decrease in metal dispersion and increase in particle size with decrease in catalytic reactivity (Table 1).

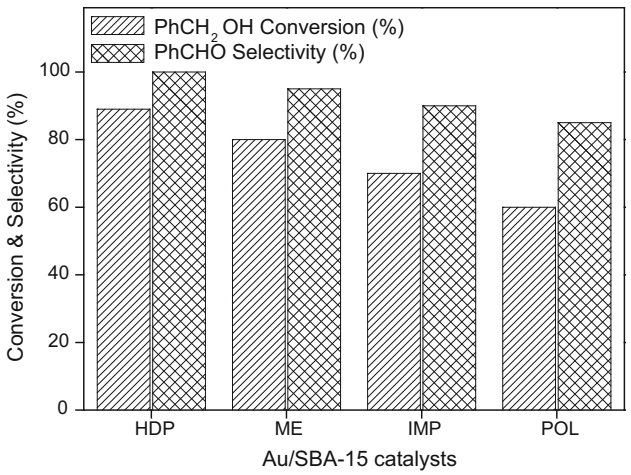

Fig. 6 Effect on $PhCH_2OH$ conversion and selectivity for PhCHO over various Au/SBA-15 catalysts, reaction conditions: weight of the catalyst = 1.0 g; reaction temperature = 320 °C; WHSV = 2.84 h^{-1}

TEM is a powerful technique to investigate the particle size of metal nanoparticles on catalytic support. The gold nanoparticles are spherical in shape and confined to the channels of the mesoporous SBA-15 as shown in Fig. 3. The corresponding histogram (Fig. 3, inset) shows the distribution of gold particles of Au/SBA-15 catalysts. The mean diameter of gold particles are found to be ~7–11 nm (TEM) while the average crystallite size of gold particles were obtained to be ~6–10 nm from XRD results are reported in Table 1. However, some of these Au nanoparticles were lying on the outside surface wall of the pores and some of the particles lying inside the pores of support which indicates the formation of strong interactions between the Au and the support

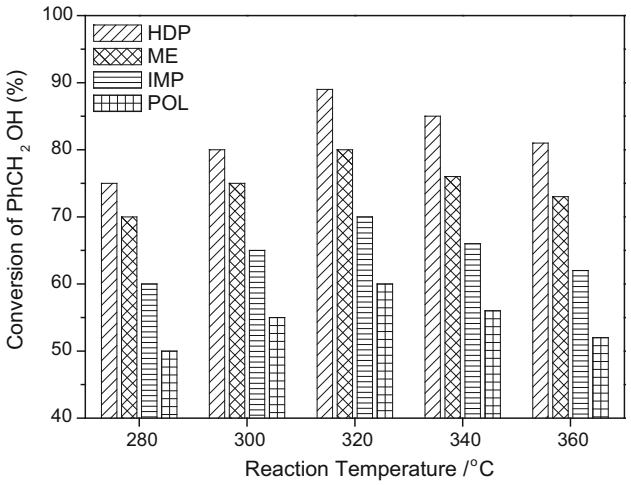

Fig. 7 Effect of temperature on $PhCH_2OH$ conversion over various Au/SBA-15, reaction conditions: weight of the catalyst = 1.0 g; WHSV = 2.84 h^{-1}

[26]. The TEM results are found to be in good agreement with results of the XRD and CO chemisorption measurements.

The nitrogen adsorption/desorption isotherms of SBA-15 and various Au/SBA-15 catalysts are shown in Fig. 4a. All the samples exhibit Langmuir type IV isotherms [27], which is a characteristic feature of mesoporous materials. SBA-15 shows a hysteresis loop which typically features a two-dimensional P6 mm structure formed by open cylindrical mesopores.

The isotherms of all Au/SBA-15 catalysts are identical to the isotherm of SBA-15. The nitrogen adsorption isotherms of SBA-15 and Au/SBA-15 catalysts exhibit H1-type hysteresis loop and features a sharp step in the P/P_0 range of 0.65–0.95, the sharpness of this step is indicative of the uniformity of the pore size [27]. However, the hysteresis loops of all Au/SBA-15 catalysts become smaller and position of the step shifts towards lower relative pressure, indicating that a smaller pore size is formed. This could be due to the deposition of Au nanoparticles in the pore of the SBA-15. Physical properties/structural parameters of the samples derived from the nitrogen isotherms are reported in Table 2 and the pore size distribution calculated from desorption branch are shown in Fig. 4b. The surface area and pore volume decreases as a result of incorporation of Au nanoparticles into the mesoporous channels of the support [28, 29].

ICP-OES analysis, performed on the fresh samples of Au/SBA-15 catalysts and the results are shown in Table 2. The prepared catalysts have shown about ~75–85 % of the expected Au loading.

In order to verify the oxidation states of gold element in as synthesized Au/SBA-15 catalysts were investigated by XPS are reported in Table 2. The XPS survey scan show the peaks characteristic of C 1 s (285 eV), O 1 s (530 eV), Si 2p (100 eV) and Au 4f (85 eV) elements. As can be seen from Fig. 5 the high resolution XPS spectrum shows binding energy of Au^0 $4f_{7/2}$ at 84.0 and Au^0 $4f_{5/2}$ at 87.7 eV, which are significantly different from Au^+ $4f_{7/2}$ (84.6 eV) and Au^{3+} $4f_{7/2}$ (87.0 eV).

The results suggest that the gold species are in the metallic state and these binding energy values correspond to the metallic gold particles [30–32]. However the XPS results confirmed the absence of any contamination from sodium and chlorine species [33]. These results further confirm that Au particles on the surface of SBA-15 support are in zero valence state. The XPS spectra of the present investigation did not show any peaks corresponding to the binding energies at 84.6 eV ($4f_{7/2}$) and 87.0 eV ($4f_{7/2}$) due to the cationic form of Au^+ and Au^{+3} oxidation states respectively. This suggests that the formation of Au metal nanoparticles takes place on the surface of SBA-15 support.

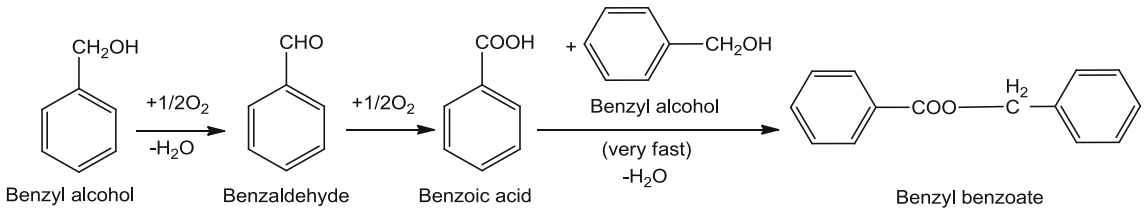

Scheme 1 Reaction pathway for the catalytic oxidation of benzyl alcohol over Au/SBA-15 catalysts

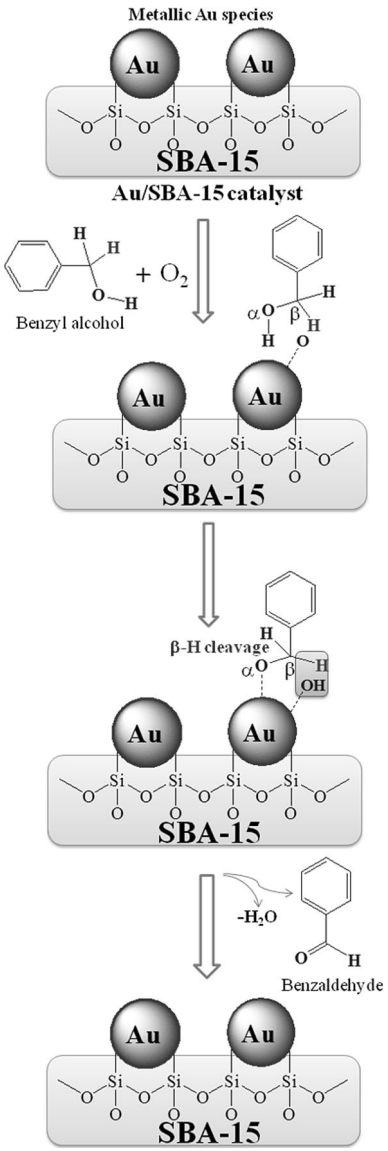

Scheme 2 Proposed reaction mechanism for the catalytic oxidation of benzyl alcohol over Au/SBA-15 catalysts

3.2 Catalytic Performance for Vapor Phase Oxidation of Benzyl Alcohol

The selective vapor phase oxidation of benzyl alcohol ($PhCH_2OH$) to benzaldehyde (PhCHO) with air as oxidant was employed to examine the catalytic performance of the Au/SBA-15 catalysts. In the absence of catalysts, only 5.7 % of benzyl alcohol was converted due to non-catalytic oxidation. Also, the pure SBA-15 support by itself showed a poor catalytic activity under the similar reaction conditions.

3.2.1 *Effect of Preparation Methods*

The catalytic activity in terms of $PhCH_2OH$ conversion and selectivity for PhCHO over various Au/SBA-15 catalysts are shown in Fig. 6. The effect of catalysts preparation method was investigated over oxidation of benzyl alcohol. The Au/SBA-15 catalyst from HDP method showed a higher activity as well as selectivity for PhCHO compared to the catalysts prepared by other methods. However, the catalytic properties reveal that negligible amounts of benzoic acid (PhCOOH), benzyl benzoate ($PhCH_2O_2CPh$), benzene (PhH) and toluene ($PhCH_3$) are formed as by-products with catalysts prepared by ME, IMP and POL methods. The decrease in the conversion of benzyl alcohol is probably due to lesser number of active gold sites on the mesoporous SBA-15 surface was available. This further suggests the promotion of agglomerization of gold nanoparticles and confirmed from XRD and TEM results. The enhanced catalytic activity was probably attributed to high dispersion of gold particles of smaller size on the mesoporous SBA-15 support.

3.2.2 *Effect of Reaction Temperature*

The effect of temperature on the vapor phase oxidation of $PhCH_2OH$ was carried out at different temperatures in the range 280–360 °C over Au/SBA-15 catalysts as shown in Fig. 7. The results suggest that below 280 °C no oxidation reaction of $PhCH_2OH$ takes place and above 360 °C, the product undergoes faster thermal degradation along with agglomerization of gold nanoparticles [1]. However, at 320 °C, the Au/SBA-15 (HDP) catalyst shows a maximum conversion of $PhCH_2OH$ up to 90 % as compared to the other three supported gold catalysts (Fig. 7). It is known that high reaction temperature favours complete oxidation of $PhCH_2OH$ and leads to the formation of benzoic acid

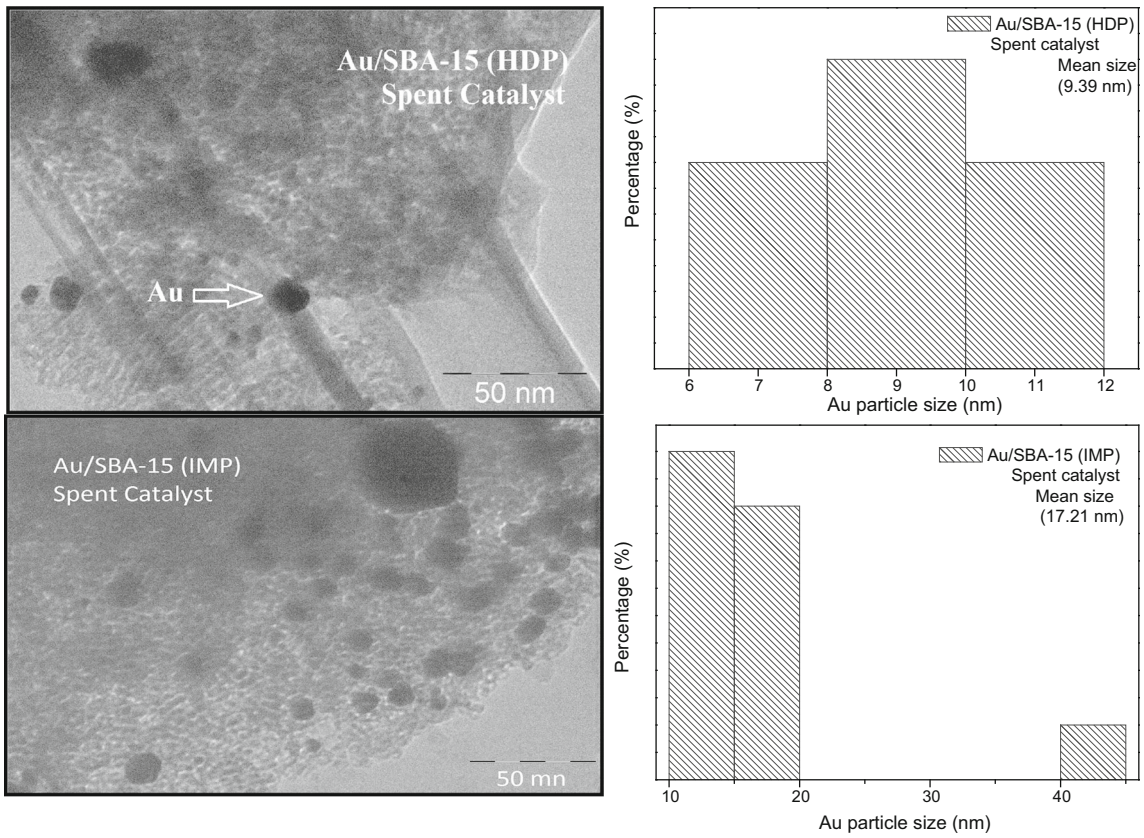

Fig. 8 TEM images of spent Au/SBA-15 catalysts

(PhCOOH) and trace amount of benzene (PhH) and toluene ($PhCH_3$) as a by-product [4, 34]. Therefore, the reaction temperature (320 °C) was considered as the optimum reaction temperature for the title reaction and also referred as trade-off between PhCHO selectivity and $PhCH_2OH$ conversion. It was interesting to note that benzyl benzoate is the only other product formed apart from PhCHO and the formation of benzoic acid (PhCOOH) was not at all detected in GC and GC-MS analysis [5]. The absence of benzoic acid in the reaction product indicates that, as soon as PhCHO was formed, it reacts immediately with $PhCH_2OH$, which was available in much higher concentration, forming benzyl benzoate as the by-product and the following reaction mechanism [34] is represented in the Scheme 1. Here the following esterification reaction was generally an acid catalyzed reaction. The mesoporous SBA-15 support is mildly acidic [10] and hence it favors to undergo corresponding esterification reaction.

3.2.3 Time-On-Stream (TOS) Analysis

The time on stream analysis on Au/SBA-15 catalysts were investigated to understand the stability of catalysts during benzyl alcohol oxidation reaction. The conversion of $PhCH_2OH$ and the product selectivity were monitored at different reaction intervals. In order to estimate the catalyst life in the present study the time on stream analysis was carried out at optimum reaction temperature of 320 °C. The gas analysis suggests that CO, CO_2 were not detected under the reaction condition (in the range of reaction temperature up to 320 °C). The benzyl alcohol conversion showed an optimum conversion after 2 h over Au/SBA-15 (HDP) catalyst as compared to other three Au/SBA-15 catalysts prepared by ME, IMP and POL methods. Further increase in the reaction time, showed a decreased $PhCH_2OH$ conversion. The supported gold catalyst needs induction period (at least 2 h) to reach its optimal catalytic activity. The presence of induction period indicates that the metallic gold nanoparticles on the catalyst surface are required to be activated at the initial stage and the oxygen molecules adsorbed on the metallic gold. Further it was dissociated to create an oxidized gold surface for the oxidation of benzyl alcohol and a possible mechanism was proposed as shown in Scheme 2. The proposed mechanism for the oxidation of benzyl alcohol over the Au/SBA-15 catalysts with slight modification done from the earlier reported [35, 36]. Based on the reaction route, to increase the conversion of $PhCH_2OH$, the reaction time needs to be

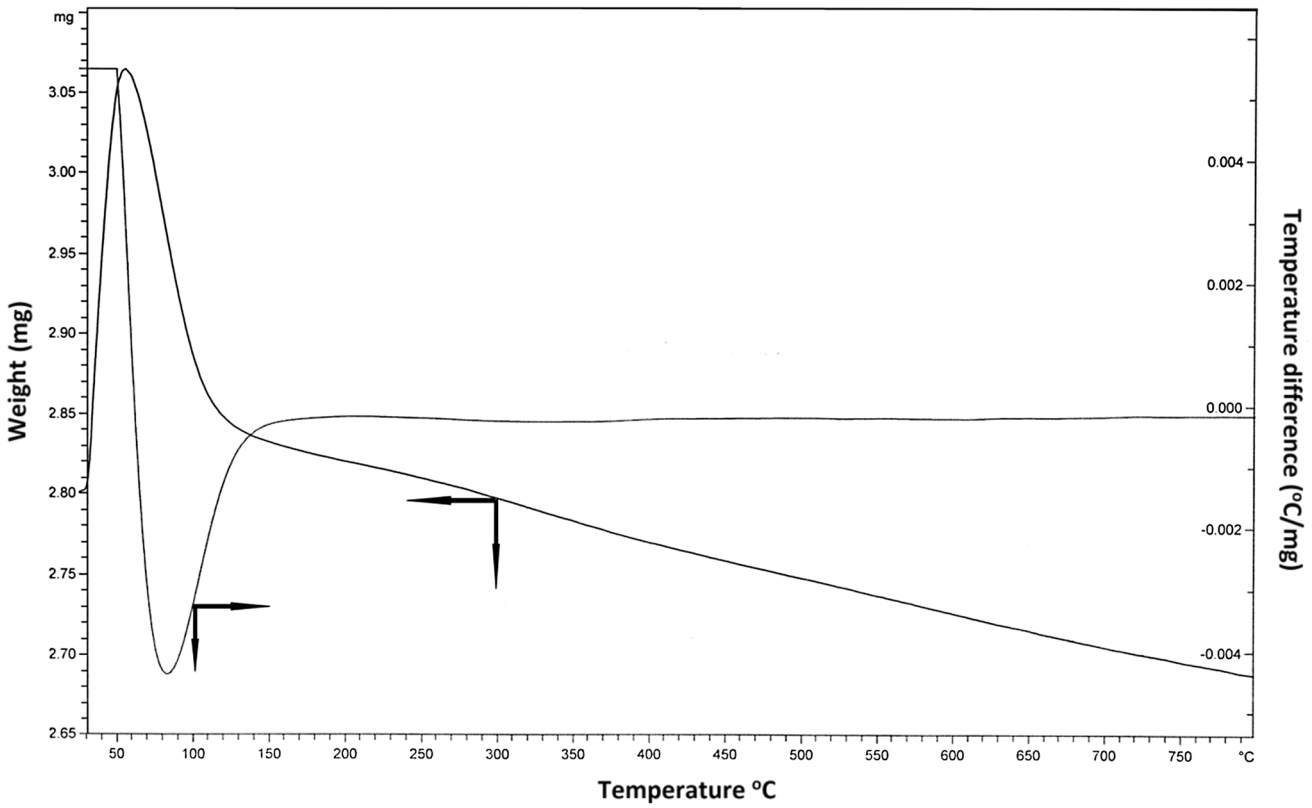

Fig. 9 TGA analysis of spent Au/SBA-15 (HDP) catalysts

prolonged. However, the PhCHO selectivity decreases due to subsequent reaction of benzaldehyde to benzyl benzoate. There was no significant difference in the $PhCH_2OH$ conversion with increase of the reaction time beyond 2 h. Whereas the PhCHO selectivity decreased continuously. The PhCHO selectivity of 80 % was attained at 12 h, while that of benzyl benzoate (a by-product) increased to 20 %. After 2 h, the conversion reaches a constant value of more than 70 %.

To understand the deactivation of the catalyst, TEM and TGA analysis was carried out over spent catalysts, as shown in Figs. 8 and 9 respectively. These results suggest that either the particle size of gold becomes larger during the course of the reaction causing the deactivation to occur or due to carbon deposition over Au/SBA-15 catalysts. To confirm this, an experiment was carried out on the spent catalyst (after the reaction run 360 °C) which was recalcined at 400 °C for 4 h in air. On this calcined sample, a fresh experiment was carried under similar reaction conditions (WHSV = 2.84 h^{-1} and T = 320 °C). Interestingly, it was observed that the activity of this catalyst was much lower than the earlier reaction carried out on the fresh catalyst under identical conditions at 320 °C. This suggests that the decrease in oxidation activity is not due to coke deposition but due to agglomeration of smaller gold nano particles to larger size gold particles. TEM and TGA analysis further confirmed that the particle size of gold becomes larger during the course of the reaction and there is no coke deposition over Au/SBA-15 catalysts respectively.

The $PhCH_2OH$ activity results suggest that Au/SBA-15 catalyst prepared by HDP method is highly an efficient method for the vapour phase oxidation of benzyl alcohol to benzaldehyde. The reasons for faster deactivation of the catalyst may be attributed to the lower surface area and lower dispersion of larger size nano particles formed during the reaction time. The catalytic activity was correlated with the particle size of gold on Au/SBA-15 catalysts. The Au/SBA-15 catalyst prepared by ME, IMP and POL method exhibits low catalytic activity compared to Au/SBA-15 catalyst prepared by HDP method and this may be attributed to the decrease in the number of active sites of gold on SBA-15 due to agglomeration of gold nanoparticles as evidenced from TEM results.

4 Conclusions

Au nanoparticles supported on SBA-15 were prepared by HDP method shows a higher catalytic performance in terms of benzyl alcohol activity and selectivity for benzaldehyde as compared to the other three Au/SBA-15

catalysts prepared by ME, IMP IMP and POL method. XRD and pore size distribution confirm that the pore structure remains intact even after the insertion of gold nanoparticles into the SBA-15 mesoporous support. XPS results reveal that the nanoparticles of gold are present in the metallic state (Au^0), which is further supported by TEM and CO-chemisorption measurements. The high performance of Au/SBA-15 catalyst makes it a promising catalytic material for the oxidation of benzyl alcohol.

Acknowledgments Ashish Kumar thanks University Grants Commission (UGC), New Delhi, India, for the award of Senior Research Fellowship (SRF).

References

1. Pina CD, Falletta E, Rossi M (2008) J Catal 260:384–386
2. Enache DI, Edwards JK, Landon P, Solsona-Espriu B, Carley AF, Herzing AA, Watanabe M, Kiely CJ, Knight DW, Hutchings GJ (2006) Science 311:362–365
3. Haruta M (2002) Cattech 6:102–115
4. Enache DI, Knight DW, Hutchings GJ (2005) Catal Lett 103:43–52
5. Choudhary VR, Dumbre DK (2009) Top Catal 52:1677–1687
6. Biella S, Rossi M (2003) Chem Commun 21:378–379
7. Choudhary VR, Dumbre DK, Bhargava SK (2009) Ind Eng Chem Res 48:9471–9478
8. Chen Y, Lim H, Tang Q, Gao Y, Sun T, Yan Q, Yang Y (2010) Appl Catal A 380:55–65
9. Zhao D, Feng J, Huo Q, Melosh N, Fredrickson GH, Chmelka BF, Stucky GD (1998) Science 279:548–552
10. Deng Y, Wei J, Sun Z, Zhao D (2013) Chem Soc Rev 42:4054–4070
11. Ariga K, Vinu A, Yamauchi Y, Ji Q, Hill JP (2012) Bull Chem Soc Jpn 85:1–32
12. Tran ND, Besson M, Descorne C (2011) New J Chem 35:2095–2104
13. Lopez N, Nørskov JK, Janssens TVW, Carlsson A, Molina AP, Clausen BS, Grunwaldt JD (2004) J Catal 225:86–94
14. Tsubota S, Haruta M, Kobayashi T, Ueda A, Nakahara Y (1991) Stud Surf Sci Catal 63:695–704
15. Widmann D, Behm RJ (2011) Angew Chem Int Ed 50:10241–10245
16. Pavankumar V, Srikanth CS, Rao AN, Chary KVR (2014) J Nanosci Nanotechnol 14:3137–3146
17. Kumar A, Kumar VP, Vishwanathan V, Chary KVR (2014) Mater Res Bull 61:105–112
18. Venugopal A, Scurrell MS (2003) Appl Catal A 245:137–147
19. Chary KVR, Srikanth CS, Rao VV (2009) Catal Commun 10:459–463
20. Chary KVR, Srikanth ChS (2009) Catal Lett 128:164–170
21. Wang H, Wang JG, Shen ZR, Liu YP, Ding DT, Chen TH (2010) J Catal 275:140–148
22. Devarajan S, Bera P, Sampath S (2005) J Colloid Interface Sci 290:117–129
23. Hu LH, Ji SF, Jiang Z, Song HL, Wu PY, Liu QQ (2007) J Phys Chem C 111:15173–15184
24. Wang HP, Liu CJ (2011) Appl Catal B 106:672–680
25. Chen Y, Wang H, Liu CJ, Zeng Z, Zhang H, Zhou C, Jia X, Yang Y (2012) J Catal 289:105–117
26. Makgwane PR, Ray SS (2013) J Mol Catal A 373:1–11
27. Yang HW, Tang DL, Lu XN, Yuan YZ (2009) J Phys Chem C 113:8186–8193
28. Zhan G, Huang J, Du M, Sun D, Abdul-Rauf I, Lin W, Hong Y, Li Q (2012) Chem Eng J 187:232–238
29. Du M, Zhan G, Yang X, Wang H, Lin W, Zhou Y, Zhu J, Lin L, Huang J, Sun D, Jia L, Li Q (2011) J Catal 283:192–201
30. Wang Z, Wang XV, Zeng DY, Chen MS, Wan HL (2011) Catal Today 260:144–152
31. Hussain ST, Iqbal M, Mazhar M (2009) J Nanopart Res 11:1383–1391
32. Kumar A, Kumar VP, Kumar BP, Vishwanathan V, Chary KVR (2014) Catal Lett 144:1450–1459
33. Dimitratos N, Lopez-Sanchez JA, Morgan D, Carley A, Prati L, Hutchings GJ (2007) Catal Today 122:317–324
34. Choudhary VR, Chaudhari PA, Narkhede VS (2003) Catal Commun 4:171–175
35. Wang H, Fan W, He Y, Wang J, Kondo JN, Tatsumi T (2013) J Catal 299:10–19
36. Chen YT, Zheng HJ, Guo Z, Zhou CM, Wang C, Borgna A, Yang YH (2011) J Catal 283:34–44